Journal of Plant Physiology 231 (2018) 135–146

Contents lists available at ScienceDirect

Journal of Plant Physiology

journal homepage: www.elsevier.com/locate/jplph

Overexpression of *Cicer arietinum* βIII-Gal but not βIV-Gal in arabidopsis causes a reduction of cell wall β-(1,4)-galactan compensated by an increase in homogalacturonan

Lucía Izquierdo[a], Ignacio Martín[a], Lucía Albornos[a], Josefina Hernández-Nistal[b], Pablo Hueso[c], Berta Dopico[a], Emilia Labrador[a,*]

[a] Departamento de Botánica y Fisiología Vegetal, Centro Hispano Luso de Investigaciones Agrarias (CIALE), Universidad de Salamanca, Salamanca, 37007, Spain
[b] Departamento de Biología Funcional, Universidad de Santiago de Compostela, Lugo, 27002, Spain
[c] Departamento de Bioquímica y Biología Molecular, Universidad de Salamanca, Salamanca, 37007, Spain

ARTICLE INFO

Keywords:
Arabidopsis
β-Galactosidases
β-(1,4)-galactan
Cell wall
Cicer arietinum

ABSTRACT

In *Cicer arietinum*, as in several plant species, the β-galactosidases are encoded by multigene families, although the role of the different proteins is not completely elucidated. Here, we focus in 2 members of this family, βIII-Gal and βIV-Gal, with high degree of amino acid sequence identity (81%), but involved in different developmental processes according to previous studies. Our objective is to deepen in the function of these proteins by establishing their substrate specificity and the possible alterations caused in the cell wall polysaccharides when they are overproduced in *Arabidopsis thaliana* by constructing the 35S::βIII-Gal and 35S::βIV-Gal transgenic plants.

βIII-Gal does cause visible alterations of the morphology of the transgenic plant, all related to a decrease in growth at different stages of development. FTIR spectroscopy and immunological studies showed that βIII-Gal causes changes in the structure of the arabidopsis cell wall polysaccharides, mainly a reduction of the galactan side chains which is compensated by a marked increase in homogalacturonan, which allows us to attribute to galactan a role in the control of the architecture of the cell wall, and therefore in the processes of growth. The 35S::βIV-Gal plants do not present any phenotypic changes, neither in their morphology nor in their cell walls. In spite of the high sequence homology, our results show different specificity of substrate for these proteins, maybe due to other dissimilar characteristics, such as isoelectric points or the number of *N*-glycosylation sites, which could determine their enzymatic properties and their distinct action in the cell walls.

1. Introduction

β-galactosidases (EC 3.2.1.23) catalyze the hydrolysis of terminal galactosyl residues from carbohydrates, glycoproteins and galactolipids. They fall into four glycoside hydrolase (GH) families (Cantarel et al., 2009). GH1, GH2 and GH42 are mostly found in microorganisms, whereas GH35 enzymes are found in both prokaryotes and eukaryotes. The plant β-galactosidases have been described to belong to GH family 35.

These enzymes are widely distributed in higher plants and can be found in different plant tissues. They are encoded by multigene families in several plant species (Smith and Gross, 2000; Esteban et al., 2003; Ahn et al., 2007). Most of them have an N-terminal signal peptide, and many appear targeted to the apoplast, suggesting their potential involvement in cell wall modifications, although they may be directed to other subcellular compartments (Hobson and Deyholos, 2013; Liu et al., 2013). Cell wall β-galactosidases may act on β-(1,4) galactosyl residues of pectic galactans (McCartney et al., 2003; Sorensen et al., 2000; Martín et al., 2005), β-(1,3) and β-(1,6)-galactosyl residues in arabinogalactan proteins (Kotake et al., 2005) or β-(1,2) linked galactose of xyloglucans (Edwards et al., 1988; Sampedro et al., 2012), and their action has been reported in the degradation of cell wall components during cell wall expansion, cell senescence, fruit ripening, and storage mobilization (Dopico et al., 1990; Ross et al., 1994; Buckeridge and Reid, 1994; Wu and Burns, 2004).

Four members of the *Cicer arietinum* β-galactosidase multigene

Abbreviations: GH, glycoside hydrolase; HG, homogalacturonan; XG, xyloglucan; WT, wild type

* Corresponding author at: Departamento de Botánica y Fisiología Vegetal, Centro Hispano Luso de Investigaciones Agrarias (CIALE), Universidad de Salamanca. C/ Licenciado Méndez Nieto s/n, Salamanca, 37007, Spain.
E-mail address: labrador@usal.es (E. Labrador).

https://doi.org/10.1016/j.jplph.2018.09.008
Received 18 July 2018; Received in revised form 10 September 2018; Accepted 18 September 2018
Available online 21 September 2018

family, named *CarBGal-1, -3, -4,* and *-5*, coding for βI-Gal, βIII-Gal, βIV-Gal and βV-Gal, respectively, has been studied by our group (Esteban et al., 2005). The role of these chickpea β-galactosidases has not yet been completely elucidated. Nevertheless, the transcription pattern of these *CarBGal* genes, along with protein accumulation and immunolocalization studies, suggest different roles for their corresponding proteins throughout development (Esteban et al., 2003, 2005; Martín et al., 2005, 2008; 2009; 2011; 2013; Hernández-Nistal et al., 2014).

The proteins deduced from the chickpea *CarBGal* genes have a high level of amino acid sequence identity with one another. βIII-Gal and βIV-Gal are the closest at amino acid sequence level (81% identity), but despite this high sequence identity, previous studies on these two proteins have pointed to distinct roles in different developmental processes.

βIII-Gal protein, responsible for the cell wall autolytic process (Dopico et al., 1989), has been related to cell wall changes during elongation processes and its function in the degradation of β-(1,4)-galactan chains was confirmed after the transformation of potato plants with the chickpea *CarBGal-3* (Esteban et al., 2003; Martín et al., 2005). Besides this role in cell wall loosening, βIII-Gal may act on sieve elements, contributing to cell wall reinforcement and allowing phloem elements to differentiate, even early in development (Martín et al., 2013; Hernández-Nistal et al., 2014).

On the other hand, βIV-Gal has been related to cell wall modifications leading to a decreased elongation rate, both in seedlings and plants, as indicated by the accumulation of *CarBGal-4* transcripts and βIV-Gal protein in most aged epicotyls and basal stem internodes, both undergoing low elongation rates (Esteban et al., 2003; Martín et al., 2008). Furthermore, this protein is mainly located in cell types whose walls are thickening, such as vascular tissues or fibres, where it may be contributing to the stiffening of the primary cell wall or allowing secondary cell wall deposition, giving mechanical strength to the tissues in which they are located.

Considering these differences between βIII-Gal and βIV-Gal and the above mentioned sequence identity, the main objective of this work is to deepen in the function of these 2 members of the chickpea β-galactosidase family establishing how they act on the cell wall and the possible alterations caused when they are overproduced in *Arabidopsis thaliana*. To achieve this, transgenic *A. thaliana* plants overexpressing *C. arietinum CarBGal-3* or *CarBGal-4* ORFs (coding for βIII-Gal and βIV-Gal, respectively) have been generated. After the morphological characterization of these transgenic plants, the possible variations in their cell walls have been analyzed. Changes in the structure of wall polysaccharides have been established by FTIR spectroscopy, whereas alterations in the content and distribution of the various cell wall polysaccharides have been analyzed by immunological techniques, using specific antibodies against different cell wall polymers. Furthermore, we have produced them in a heterologous system in order to obtain these β-galactosidases in large quantity and in active form to carry out substrate specificity studies.

2. Material and Methods

2.1. Plant material and growth conditions

Arabidopsis thaliana ecotype Col-0 was used as host for genetic transformation. Seeds were surface sterilized as described by Albornos et al. (2012) and cold treated at 4 °C for 3 d before sowing. Seeds were grown in Petri dishes on one-half-strength Murashige and Skoog (Murashige and Skoog, 1962) agar medium with 1% (w/v) sucrose. These plates were maintained in a growth chamber (*Aralab*, Sintra, Portugal) at 22ºC with both a 16-h photoperiod (provided by cool-white fluorescent tubes at a light intensity of approximately 80-100 $\mu E/m^2/s$), or in darkness to obtain etiolated seedlings. To obtain adult plants, 10-d-old green seedlings were transferred to plastic pots containing a 3:1 mixture of potting soil and vermiculite and grown under the same conditions.

Nicotiana benthamiana plants were also used in this work. For agroinfiltration experiments, *N. benthamiana* seeds were sown in potting soil and allowed to grow for 6 weeks in a growth chamber (Aralab) at 25 °C and 16-h photoperiod.

2.2. Construction of expression vectors for Arabidopsis thaliana transformation

Constructs for arabidopsis transformation were prepared using Gateway® cloning technology (Invitrogen, USA), according to manufacturer´s instructions. *Cicer arietinum CarBGal-3* and *CarBGal-4* open reading frames (ORF) were PCR amplified adding the *att*B1 and *att*B2 sequences to the 5′- and 3′-ends, respectively. The amplified products were gel purified and used in BP reaction with pDONR201 and the entry clones generated were used in LR reaction with the pGWB2 vector (kindly provided by Professor Tsuyoshi Nakagawa) driven by *35S* promoter. All constructs were verified by sequencing. The primers used for each clone are listed on supplemental tables S2.

All constructs generated were electroporated into *Agrobacterium tumefaciens* strain C5851 m. *A. thaliana* ecotype Col-0 plants were transformed by the *Agrobacterium*-mediated floral dip method (Clough and Bent, 1998). Seeds harvested from infiltrated plants were screened on the appropriate antibiotic and resistant seedlings (T_1) were selected.

Single insertion transformant T_2 plants were screened by Southern blot according to the method described by Esteban et al. (2005). Wild type *A. thaliana* (ecotype Col-0) plants were used as negative control. gDNA was digested with *Hin*d III (with a single recognition site outside ORF in transferred DNA), and hybridized with a 913 bp PCR-amplified *CarBGal-3* ORF fragment and the complete *CarBGal-4* ORF. Different individual lines, both with single and double insertion of the transgene, were selected and screened for homozygosis. Expression levels of the transgene were determined by reverse-transcription PCR (RT-PCR) from cDNA synthesized from total RNA of 10-day-old arabidopsis transgenic and WT plantlets (used as negative control). A specific primer set for arabidopsis actin-2 gene (*ACT-2*, At3g18780) was used as internal control. The primers used for RT-PCR are listed on supplemental table S1.

2.3. Construction of expression vectors for agroinfiltration of Nicotiana benthamiana leaves

For heterologous expression in *N. benthamiana* leaves, the pDONR201 entry clones carrying the *CarBGal-3* and *CarBGal-4* ORF (generated as stated above) were used in LR reaction with the pEAQ-HT-DEST1 vector (Sainsbury et al., 2009; provided by Plant Bioscience Ltd, Norwich, UK). The expression constructs and the GFP-containing pEAQ-GFP-HT vector used as control (also provided by Plant Bioscience Ltd, Norwich, UK) were transformed by electroporation into *Agrobacterium tumefaciens* strain AGL1.

For agroinfiltration experiments, 5 ml of a saturated culture of *A. tumefaciens* transformed with each construct were used to inoculate 200 ml of fresh Luria-Bertani medium. This culture was grown at 28 °C for 24 h and cells were harvested by centrifugation at 2500xg for 15 min at 4 °C and resuspended in 200 ml of infiltration solution [10 mM $MgCl_2$, 10 mM MES (2- (*N*-Morpholin) ethanesulfonic acid) and 100 μM acetosyringone]. Plants of *N. benthamiana* to be agroinfiltrated were grown in pots (1 seedling per pot) for 6 weeks under the conditions already described. Three leaves per plant of a total of 5 or 6 plants were infiltrated with each construct, using 10 ml of the suspension of the agrobacteria per plant. The suspension was pressure infiltrated into the abaxial side of *N. benthamiana* leaves by using a 1 ml syringe without needle, until the infiltration liquid reached 2/3 of the leaf surface. Plants were kept in the same growth conditions described above for 4, 6 and 12 d before leaves were collected.

2.4. Cell wall purification

The cell walls were obtained as described in Moneo-Sánchez et al. (2018) from the alcohol insoluble residue (AIR) of 3-day-old transgenic and WT seedlings grown in light and darkness conditions. The material was frozen in liquid nitrogen and grinded using a Retsch mill MM400. Methanol was added to each sample and boiled for 10 min to obtain the AIR. The walls obtained were dried at room temperature to constant dry weight.

2.5. FTIR spectroscopy and multivariate analysis

For the FTIR spectroscopic measuring, the tablets prepared in a Specadie kit (Smiths Industries, London, UK) by mixing solid samples (3 mg of cell walls obtained as described above) with KBr (100 mg) were used. The spectra were recorded on a Bomen MB 160 FTIR spectrometer (Hartmann and Braun) at a resolution of 4 cm^{-1}, with 64 interferograms of three independent WT/transgenic line samples co-added for a high signal to noise ratio in the spectral range of 2000-900 cm^{-1}, to identify changes in cell wall polysaccharides. All spectra were normalized using Perkin-Elmer IR Data software, baseline corrected and area-normalized using the application Win-DAS (John Wiley and sons Ltd, Hoboken, NJUSA). Then the spectra were exported to Microsoft Excel 2010 for digital subtraction of transgenic and WT data. Cluster analysis based in the Euclidean distance of the different types of plants according to the UPGMA (Unweighted Pair Group Method with Arithmetic Mean) method and principal component analysis (PCA) were performed using the software IBM SPSS Statistics 20 (IBM)

2.6. Xyloglucan extraction and quantification

For xyloglucan extraction, polysaccharides from AIR of 3-day-old transgenic and WT seedlings grown in light and darkness were sequentially fractionated with water, 50 mM EDTA (pH 7.5) and 4 M KOH containing 1% w/v $NaBH_4$. Xyloglucan content was determined in the KOH fraction according to the method of Kooiman (1960). The absorbance was determined at 640 nm after incubation for 1 h at room temperature using tamarind (*Tamarindus indica*) xyloglucan as standard.

2.7. Immunofluorescence labelling of β-(1,4)-galactan and homogalacturonan

Immunofluorescence labelling of β-(1,4)-galactan and homogalacturonan was conducted with monoclonal antibody LM5, specific for four consecutive β-(1,4)-galactan residues (Jones et al., 1997) and with LM18, which recognizes partially methyl esterified HG. The labelling was performed on the first and the third floral stem internodes from 24 to 30-day-old arabidopsis plants and in rosette leaves from 17-old-day plants. Sample preparation and incubation with antibodies were performed as described in Martín et al. (2013). LM5, LM18 and secondary antibody (Goat anti rat-IgG conjugated with FITC) were applied at 1:25 and 1:50 dilutions respectively. Images were taken using a DM4000 microscope equipped with a DFC550 camera (Leica, Wetzlar, Germany).

2.8. Protein extraction and enzymatic activity of the cell wall β-galactosidases

Cell wall proteins were isolated from *N. benthamiana* leaves 4, 6 and 12 d after the inoculation. Frozen plant material (10 *g*) was grinded (30 Hz for 2 min) in a retschmill MM400 (Sarstedt, Nümbrecht, Germany), resuspended on 15 ml of 50 mM NaCl at 4 °C and centrifuged (3000x*g*, 4 °C, 15 min). The pellet was washed with acetone at -20 °C and cold 50 mM NaCl and centrifuged after each wash. To obtain the cell wall proteins, the last pellet was suspended in 1 M NaCl dissolved in 10 mM Na-citrate phosphate buffer, pH 5.5, at 4 °C for 48 h, centrifuged (3000x*g*, 15 min), and the supernatant was dialysed for 48 h using 20 mM Na-acetate buffer, pH 5.0. The protein extract was concentrated by ultrafiltration in Vivaspin 4 tubes (Sartorius Stedim, Göttingen, Germany) to a final volume of 0.2 - 0.3 ml.

The total amount of proteins was measured with the Protein assay (Bio-Rad, Hercules, USA). The hydrolytic activity of the proteins was tested using p-nitrophenyl (pNP) derivatives as substrates, basically as described in Dopico et al. (1989). The assay was performed with 4 µg of cell wall protein and 3 mM pNP substrates (pNP-α-L-arabinofuranoside, pNP-α-L-fucopyranoside, pNP-α-D-galactopyranoside, pNP-β-D-galactopyranoside, pNP-α-D-glucopyranoside, pNP-β-D-glucopyranoside, pNP-β-D-mannopyranoside, pNP-β-D-xylopyranoside, from Sigma, St Louis, USA). Incubation took place at 34 °C for 60 min. The free p-nitrophenol concentration was determined by measuring the absorbance at 400 nm using a Jenway 7315 spectrophotometer (Stone, UK). Cell wall proteins activity was also assayed against lupin β-(1,4)-galactan pretreated with α-L-arabinofuranosidase and a mix of xyloglucan oligosaccharides containing β-(1,2)-galactose (Megazyme, Wicklow, Ireland); β-(1,4)-galactobiose, larch wood arabinogalactan and lactose (Sigma, St Louis, USA); β-(1,3)-galactan, β-(1,3)(1,6)-galactan, β-(1,3)-galactobiose, β-(1,3)-galactotriose, β-(1,6)-galactobiose and β-(1,6)-galactotriose (kindly supplied by Dr. T. Kotake, Saitama University, Japan). The reaction mixture consisted of 80 µl 0.1 M sodium acetate/acetic acid buffer, pH 4.0, 80 µl enzyme solution containing 2 µg total protein and 40 µl of 0.5% (w/v) polysaccharide substrate or 5 mM oligosaccharide substrates. Samples were incubated at 37 °C for up to 24 h, and the reaction was stopped by adding 800 µl of ethanol at -20 °C. After 48 h of precipitation at -20 °C, the samples were centrifuged at 4000x g, 15 min at 4 °C. The supernatant was vacuum dry and the released sugars dissolved in 10 µl of deionized water. The reaction products were separated by thin layer chromatography on silicagel plates (Merck, Darmstadt, Germany) according to Bosch-Reig et al. (1992). The plates were sprayed with the detection reagent (0.1% orcinol in 50% sulphuric acid) and heated to 100 °C for 5 min. The galactose released was quantified in a CS-9000 Dual-wavelength Flying-spot scanner densitometer (Shimadzu, Tokyo, Japan), using commercial galactose (Sigma, St Louis, USA) as standard. Activity of βIII-Gal and βIV-Gal was estimated by subtracting the activity of leaves transformed with the GFP construct.

2.9. Statistical analysis

The data are presented as means ± standard errors (SE) of at least three biological replicates. The SPSS statistics 20 (IBM) was used for statistical analysis. Student's *t*-test was applied to compare means between transgenic and wild type plants. A significant level was set at $\alpha = 0.05$, $\alpha = 0.01$ and *** $\alpha = 0.001$.

3. Results

3.1. Selection of homozygous single insertion line

After transformation and selection of arabidopsis 35S::βIII-Gal and 35S::βIV-Gal transgenic plants, different lines in T_2 generation were analysed by Southern blot to determine the number of transgene insertions in their genome (Supplementary Fig. S1). Different individual lines, both with single and double insertion of the transgene, were selected and screened for homozygosis.

Transgene transcript accumulation in 35S::βIII-Gal and 35S::βIV-Gal selected homozygous T_3 lines was determined by RT-PCR using specific primer sets (Supplementary Table S1) for *CarBGal-3* and *CarBGal-4* respectively. Transcript accumulation was detected in all the analysed lines, except in 1.6.6 and 2.3.4 (35S::βIII-Gal) and 1.2.5 (35S::βIV-Gal) (Supplementary Fig. S2). Single insertion lines 1.10.5 and 3.1.6 for 35S::βIII-Gal and 1.4.4 and 3.8.4 for 35S::βIV-Gal were selected for

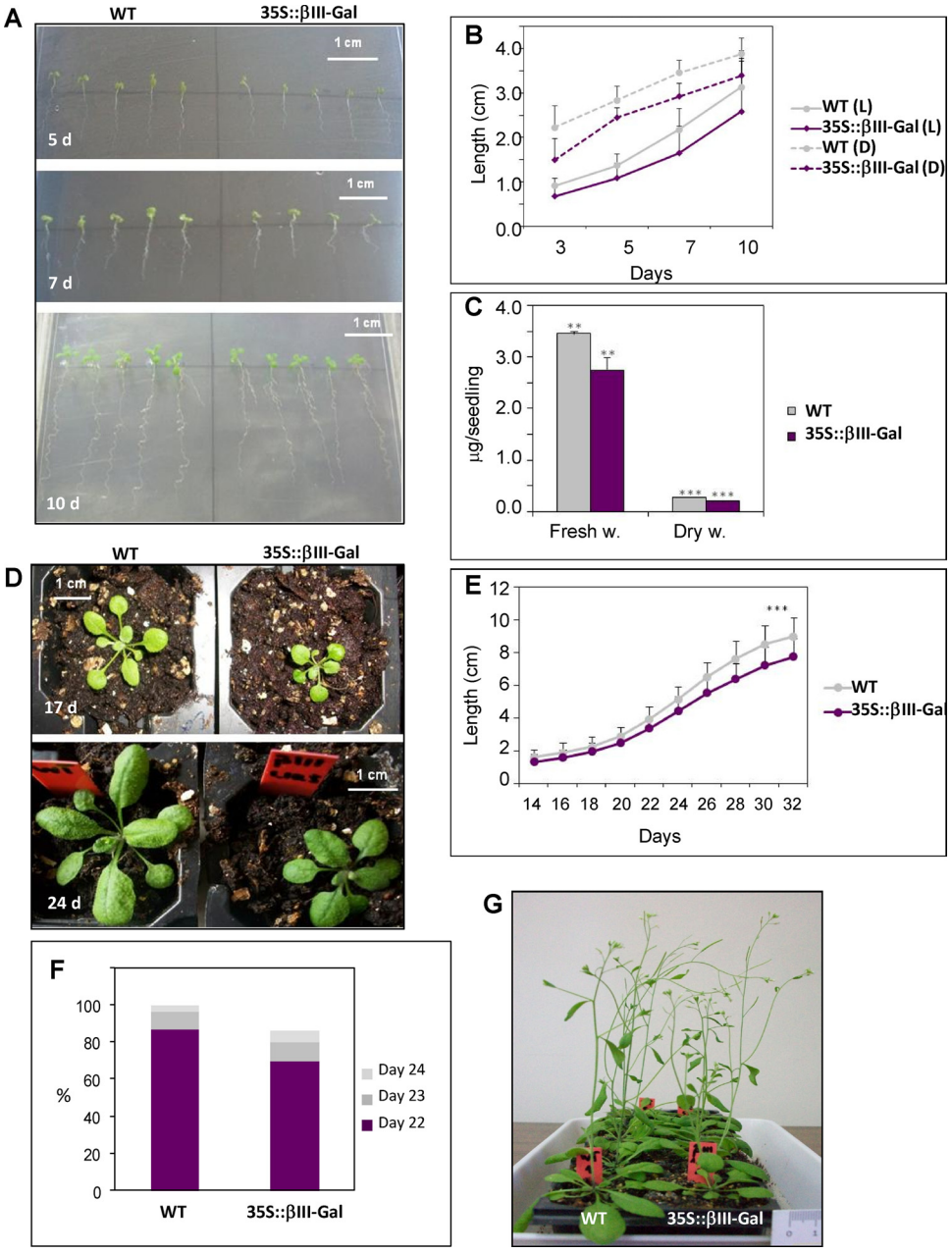

Fig. 1. Morphological changes between WT and 35S:: βIII-Gal transgenic seedlings and plants. A. 5- 7- and 10-d-old WT and 35S::βIII-Gal seedlings grown in the light. B. Length of 3- 5- 7- and 10-d-old etiolated (D) and light-grown (L) WT and 35S::βIII-Gal seedlings. C. Fresh and dry weight (w) of 10-d-old etiolated WT and 35S::βIII-Gal plants. D. 17- and 24-d-old rosettes of WT and 35S::βIII-Gal plants. E. Rosette diameter of WT and 35S::βIII-Gal plants. F. Start of bolting in WT and 35S::βIII-Gal plants. G. 32-d-old WT and 35S::βIII-Gal plants. Statistically significative differences are indicated by asteriks: * $\alpha = 0.05$, ** $\alpha = 0.01$ and *** $\alpha = 0.001$.

further analysis. Since results were similar for both lines, only data for 1.10.5 (35S:βIII-Gal) and 3.8.4 (35S:βIV-Gal) are shown. These lines will be referred hereon as 35S::βIII-Gal and 35S::βIV-Gal, respectively.

3.2. Phenotypic characterization of 35S::βIII-Gal and 35S::βIV-Gal transgenic plants

Morphological analysis: Phenotypic studies revealed a significant developmental delay in 35S::βIII-Gal plants when compared to the WT. In early development stages the transgenic lines showed smaller size regarding to WT (Fig. 1A-B), that was reflected in a significant reduction of the average fresh and dry weight per plant (Fig. 1C). The difference in size was maintained in older 17- and 24-day-old plants (Fig. 1D) with a marked reduction in rosette leaves size in 35S::βIII-Gal, that increased with the plant development (Fig. 1E). Regarding to the bolting, a slight delay was observed in 35S::βIII-Gal plants (Fig. 1F), which presented an emergence percentage of 70% at 22 days compared to 86% of WT. Once bolting has occurred no significant differences were observed during final stages of development, as can be seen in 38-day-old plants (Fig. 1G).

After a comparative study of 35S::βIV-Gal and WT plants no differences in the morphology or alterations in the growth of any of their organs could be detected (data not shown). However, as in 35S::βIII-Gal, we carried out the analysis of cell wall polysaccharides by FTIR spectroscopy and immunolocalization of galactan in order to characterize the phenotype of the plants.

Cell wall polysaccharides identification by FTIR: The FTIR cell wall spectra for the region between 2000 and 900 cm^{-1} was obtained from the alcohol insoluble residue (AIR) of 3-days-old transgenic 35S::βIII-Gal and WT plants, growing under photoperiodic conditions and in darkness (Fig. 2A) and lead us to identify characteristic peaks of the cell wall components such as cellulose (900, 1040, 1060, 1160, 1320 1367), xyloglucan (1041, 1078, 1120, 1317, 1371) and pectins (952, 1014, 1097, 1104, 1146, 1243) (Kacuráková et al., 2000; Černá et al., 2003).

In order to know possible differences between transgenic and WT plants, the spectra were compared by multivariate analysis. The

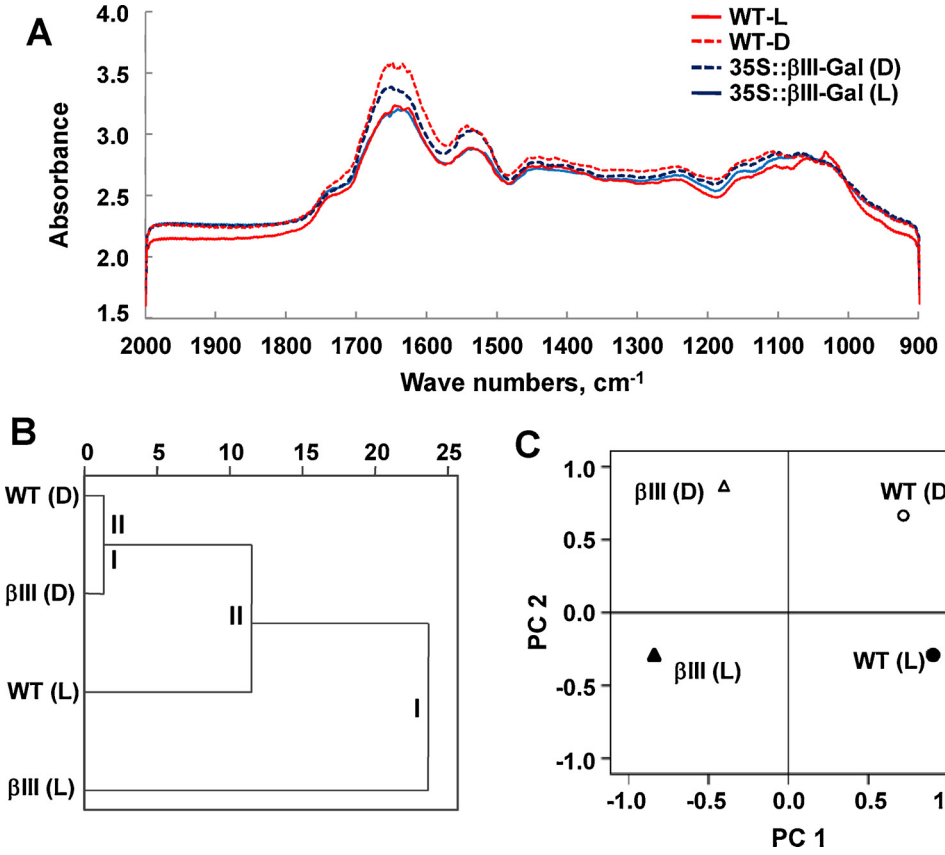

Fig. 2. A. FTIR spectra from cell wall (CW) of green (L) and etiolated (D) 3-D-old WT and 35S::βIII-Gal seedlings. B. Dendrogram generated after cluster analysis of FTIR spectra from CW of green and etiolated 3-D-old WT related to 35S::βIII-Gal seedlings. C. Principal component analysis of FTIR spectra from CW of green and etiolated 3-D-old WT related to 35S::βIII-Gal seedlings. Principal components 1 (PC1) and 2 (PC2) are shown.

dendrogram obtained (Fig. 2B) indicated that it was possible to establish three different groups that separate the 35S::βIII-Gal plants growing in light (I), the WT plant growing in light (II) and both the transgenic and WT plants growing in darkness (III). Principal components 1 and 2 (PC1 and PC2) were used to separate the four groups of spectra. PC1 and PC2, which together explain more than 96% of total covariance of data (75.10% PC1 and 21.71% PC2), allows to separate the transgenic plants with negative values for PC1 from the WT plants with positive values. Also, the light-grown plants showed negative values for the variables in the PC2, while the plants grown in darkness showed positive values (Fig. 2C).

According to the loading plots for PC1 and PC2 and the absorption assigned to different cell wall polysaccharides in the literature, our results point to a higher proportion of pectic polymers (1051, 1047, 1022 and 1014 cm^{-1}) (Černá et al., 2003; Kacuráková et al., 2000; Morris et al., 2003), galacturonic acid residues (1008 cm^{-1}) and xyloglucan (XG) (1041 cm^{-1}), the later confirmed also after XG extraction and quantification by Kooiman method (Supplementary Fig. S3), in the cell walls of transgenic plants when compared to WT (Fig. 3) as indicated by their representation in PC1 negative values. On the positive side of PC1, corresponding to WT plants, peaks corresponding to hemicellulose polysaccharides such as glucomanan (1092 cm^{-1}), and galactosyl (1068 cm^{-1}) and rhamnosyl (1086 cm^{-1}) residues were found. Regarding to PC2, which separated plants growing in light or in darkness, marked differences are found in the 1750-1500 cm^{-1} region (Fig. 3A) including peaks for both esters and carboxylic acids (McCann et al., 1997) in the negative zone of PC2, thus pointing to a higher representation of esterified and non esterified pectins in light-grown seedlings, also supported by a negative peak in this component at 1014 cm^{-1} (Fig. 3B), corresponding to pectic polysaccharides. Analysis of PC2, also indicates a higher proportion of rhamnopyranosides (1055 cm^{-1}) and rhamnogalacturonan (1045 cm^{-1}) in plants growing in darkness, as they appear in the positive zones of PC2 (Fig. 3B).

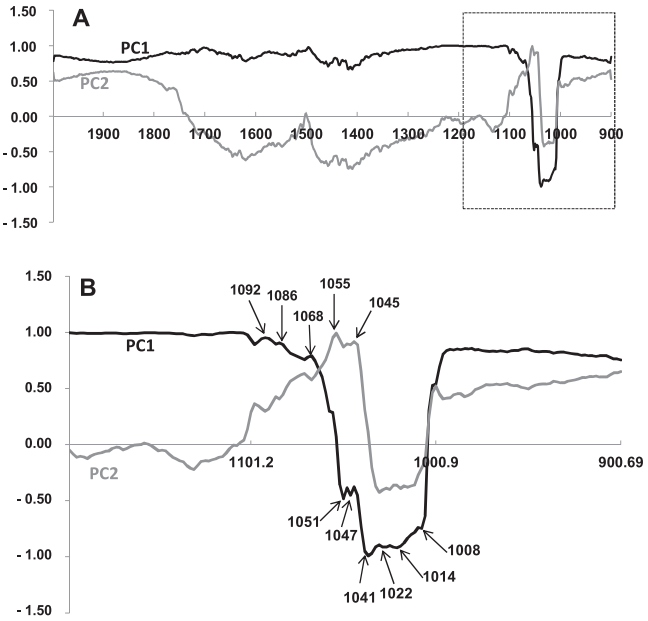

Fig. 3. A. Loading plots of principal component 1 (PC1, black line) and principal component 2 (PC2, grey line) from FTIR spectra from CW of green and etiolated 3-D-old WT and 35S::βIII-Gal seedlings. B. Amplification of the 900–1200 cm^{-1} region of FTIR spectra.

Similarly, we performed this analysis to compare 35S::βIV-Gal and WT plants. The FTIR cell wall spectra showed similar profiles (Fig. 4A), although with lower absorbance in the cell wall spectra for 35S::βIV-Gal growing in light. These spectra, as for 35S::βIII-Gal, allow us to identify characteristic peaks of the cell wall components such as cellulose, xyloglucan and pectins.

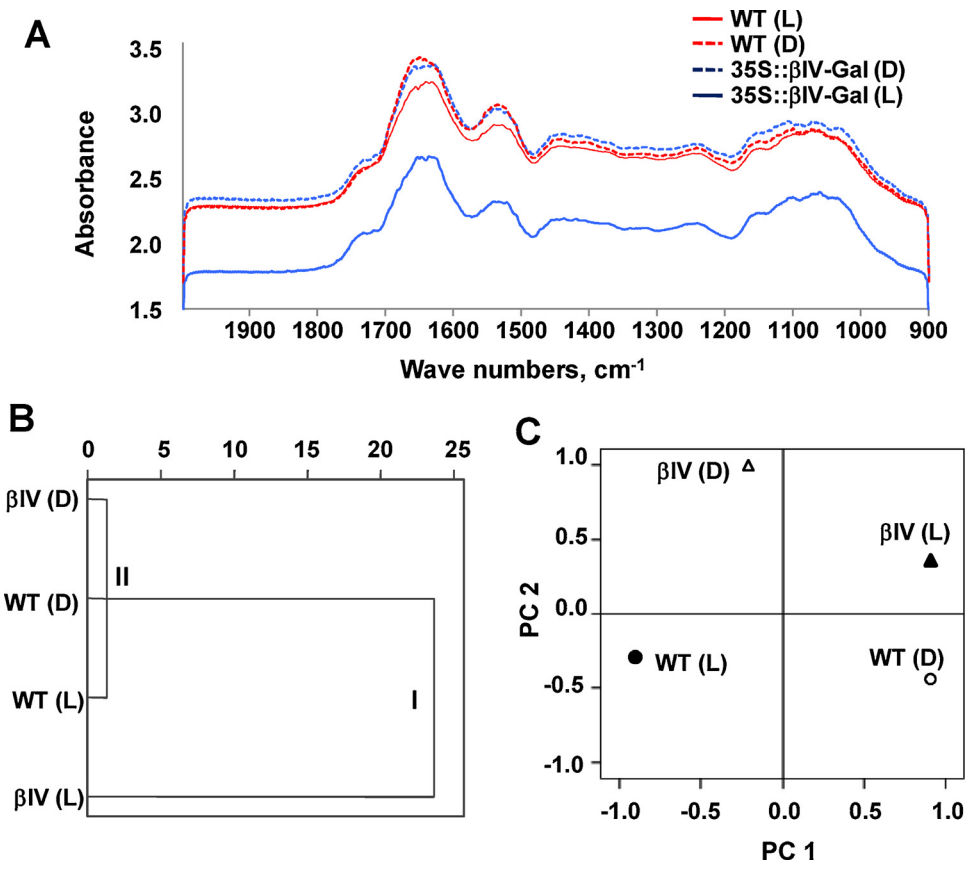

Fig. 4. A. FTIR spectra from cell wall (CW) of green (L) and etiolated (D) 3-D-old WT and 35S::βIV-Gal seedlings. B. Dendrogram generated after cluster analysis of FTIR spectra from CW of green and etiolated 3-D-old WT related to 35S::βIV-Gal seedlings. C. Principal component analysis of FTIR spectra from CW of green and etiolated 3-D-old WT related to 35S::βIV-Gal seedlings. Principal components 1 (PC1) and 2 (PC2) are shown.

When the spectra were compared by multivariate analysis, only two different groups could be established (Fig. 4B), the first (I) includes cell wall spectra of transgenic plants growing in light, while the rest of the plants are grouping in the second (II). The analysis of the principal components 1 and 2 (PC1 and PC2) indicated that PC1, which explain more than 99% of total variance of data, does not allow to separate transgenic plants from the WT plants, being the PC2, which only explains 0.54% of the covariance, the one that separates the transgenic plants from the WT plants (Fig. 4C). Thus, this analysis does not establish differences between the cell walls of 35S::βIV-Gal and WT plants related with the presence of the transgene, at least in these conditions and developmental stage.

3.3. Immunodetection of cell wall polysaccharides

In addition to morphological characterization and cell wall analysis, we conduct histological analysis to check for possible anatomical changes at the tissue level and perform immunolocalization studies to establish changes in specific polysaccharides, namely those containing four consecutive β-(1,4)-galactan residues, recognized by LM5 antibodies, and the partially methyl esterified homogalacturonan (HG) recognized by LM18. We used two stem internodes with different growth capacity, the first (basal) internode and the third (apical) internode from 28 to 32-day-old plants and the second pair of rosette leaves of 17-day-old plants.

Along the WT floral stem, the LM5 labelling intensity (Fig. 5A) changes with the degree of development, decreasing from young towards old tissues, being the labelling stronger in the apical 3rd internode, and present a higher intensity in epidermal cells, phloem cells and xylem elements. Transgenic 35S:βIII-Gal plants show a similar distribution of β-(1,4)-galactan than WT plants, although the labelling was lower in the basal 1st internode both in the cambial tissue and in the parenchyma cells. In leaves, the highest levels of β-(1,4)-galactan were found in epidermis and vascular tissues, and also in the collenchyma close to the central nerve (Fig. 5A). The labelling intensity was lower in 35S::βIII-Gal plants than in WT, mainly in epidermis and mesophyll cells, showing similar levels in vascular tissues.

The labelling distribution observed with LM18 (Fig. 5B) showed a strong increase in 35S::βIII-Gal plants regarding to WT plants in all the tissues, both in the apical and basal internodes and in leaves. The labelling intensity was similar in apical and basal internodes, and the epitopes recognized by LM18 were localized mostly in the cortical parenchyma and metaxylem cells, with a higher intensity at the cell intersection zones. In leaves, the labelling was homogeneous and no differences were detected in different tissues.

Immunolocalization studies do not allow to establish differences between WT and 35S::βIV-Gal plants (Fig. 6). Regarding to LM5 antibodies (Fig. 6A), the previously described labelling specificity depending on the cellular type and the labelling intensity according to developmental stage were observed in both types of plants, and the galactan levels in both internodes and leaves did not present significant differences between WT and transgenic plants. No differences were found either between WT and transgenic plants when immumolocalization of homogalacturonan was analysed by LM18 antibodies (Fig. 6B).

3.4. Production of β-galactosidases in heterologous systems and analysis of enzymatic activity

To establish their substrate specificity, βIII-Gal and βIV-Gal were transiently expressed in *Nicotiana benthamiana* leaves by agroinfiltration using the pEAQ/AGL1 system described in Materials and Methods. SDS-PAGE of cell wall protein extracts from infiltrated leaves harvested at different times showed the highest production levels of both βIII-Gal and βIV-Gal proteins at 6-d post-infiltración (data not shown). The produced βIII-Gal and βIV-Gal were active against pNP-β-D-

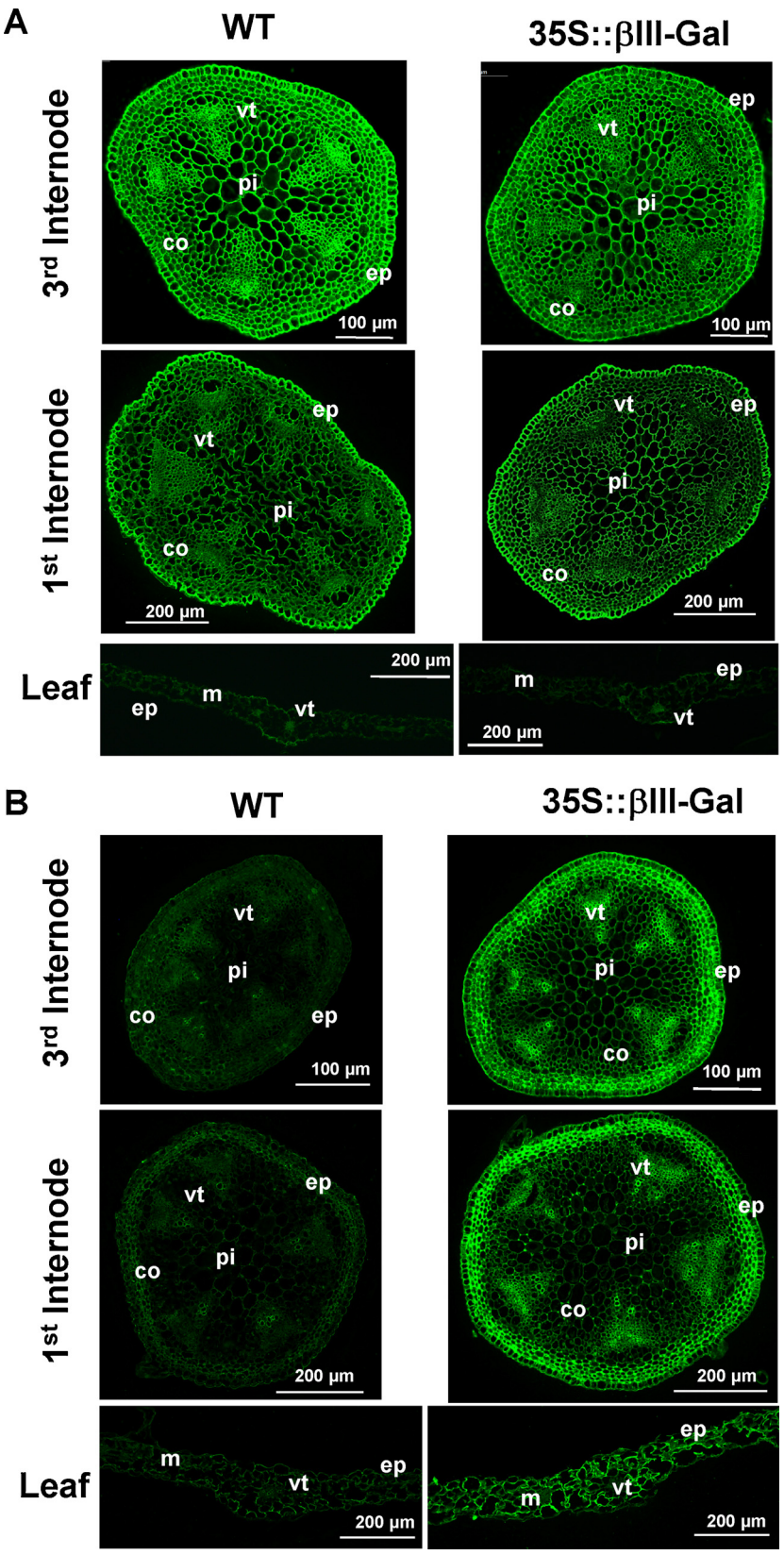

Fig. 5. Immunolocalization of A: β-D-(1,4)-galactan (LM5) and B: Homogalacturonan (LM18) in 3rd (apical) and 1st (basal) internodes and in rosette leaves of WT and 35S::βIII-Gal transgenic plants. co, cortex, ep, epidermis, m: mesophyll, pi, pith, vt, vascular tissue. Scale bars = 100 and 200 µm.

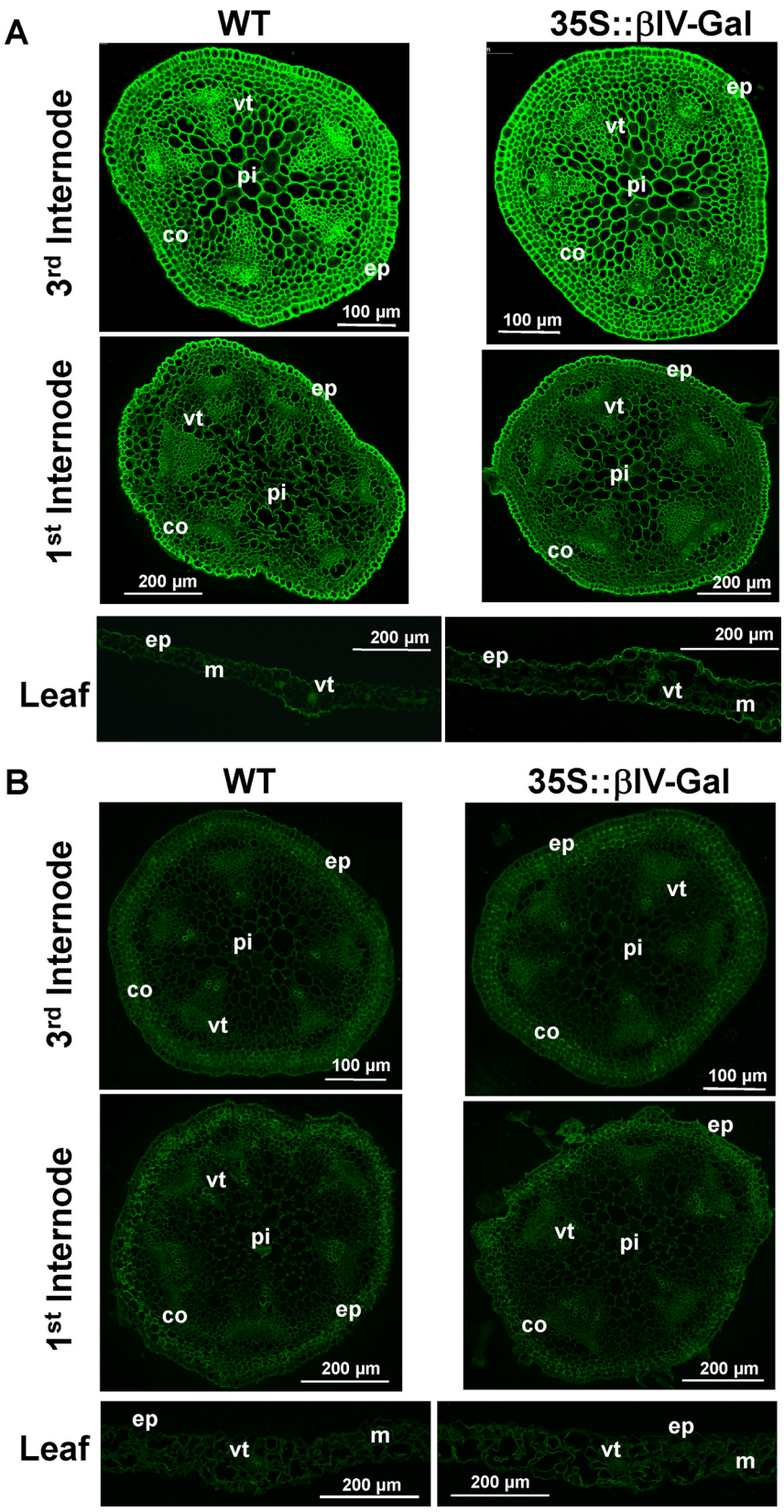

Fig. 6. Immunolocalization of A: β-D-(1,4)-galactan (LM5) and B: Homogalacturonan (LM18) in 3rd (apical) and 1st (basal) internodes and in rosette leaves of WT and 35S::βIV-Gal transgenic plants. co, cortex, ep, epidermis, m: mesophyll, pi, pith, vt, vascular tissue. Scale bars = 100 and 200 µm.

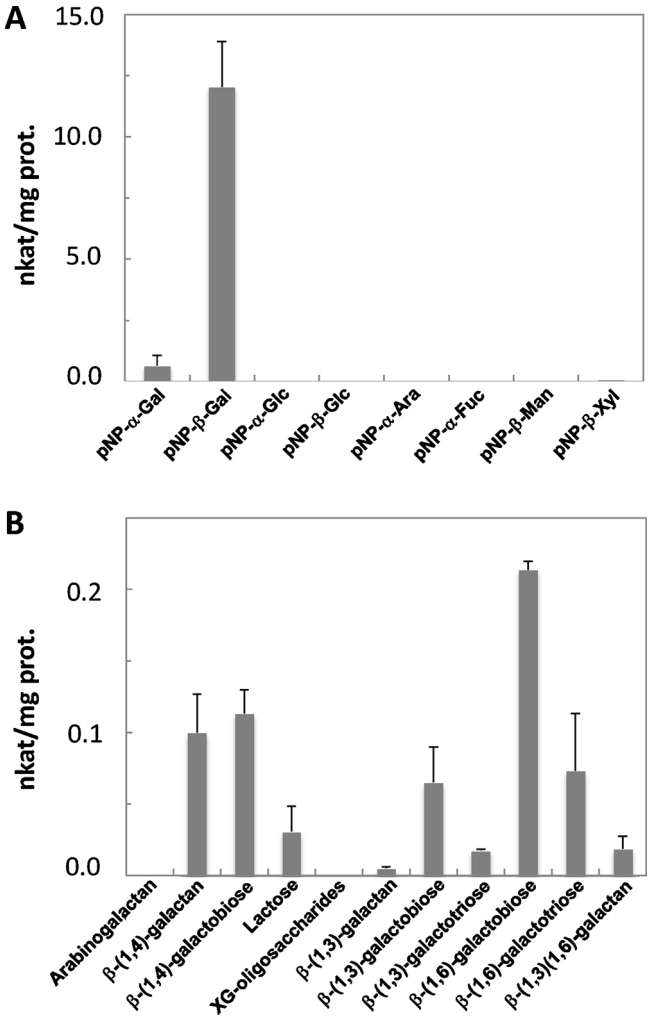

Fig. 7. Activity against several substrate of the chickpea βIII-Gal produced 6 d after agroinfiltration of *N. benthamiana* leaves. A. Hydrolytic activity of the proteins using p-nitrophenyl (pNP) derivatives as substrates (pNP-α-D-galactopyranoside, pNP-β-D-galactopyranoside, pNP-α-D-glucopyranoside, pNP-β-D-glucopyranoside, pNP-α-L-arabinofuranoside, pNP-α-L-fucopyranoside, pNP-β-D-mannopyranoside, pNP-β-D-xylopyranoside). B. Hydrolytic activity of the protein using larch wood arabinogalactan, lupin β-(1,4)-galactan, β-(1,4)-galactobiose, lactose, a mix of xyloglucan oligosaccharides containing β-(1,2)-galactose, β-(1,3)-galactan, β-(1,3)-galactobiose, β-(1,3)-galactotriose, β-(1,6)-galactobiose, β-(1,6)-galactotriose, β-(1,3)(1,6)-galactan.

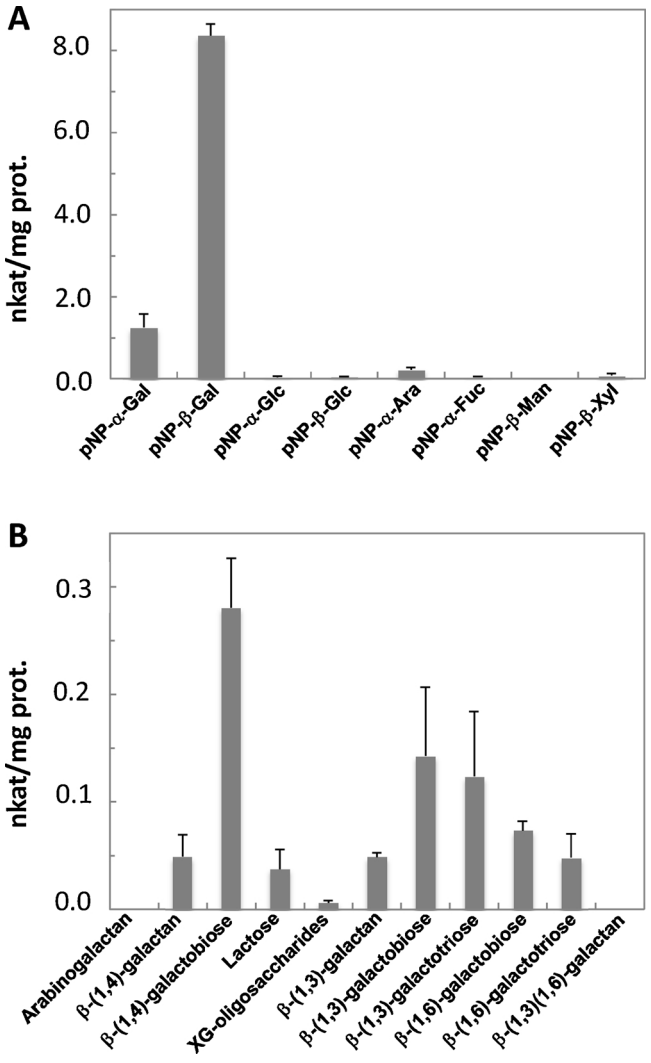

Fig. 8. Activity against several substrate of the chickpea βIV-Gal produced 6 d after agroinfiltration of *N. benthamiana* leaves. A and B as in Fig. 7.

galactopyranoside substrate, being this activity higher for βIII-Gal (Figs. 7A and 8 A). Very low activity against pNP-α-galactosidase was also detected in both cases (Figs. 7A and 8 A).

A study with different Gal- containing substrates was carried out to determine the activity of the two β-galactosidases against different linkages and polymerization degrees. βIII-Gal shows activity against β-(1,4)-galactan and β-(1,4)-galactobiose at similar levels, although only slight activity is detected against lactose. βIII-Gal is also able to hydrolize β-(1,6) and β-(1,3) linkages but only in galactobiose and to a lesser extent in galactotrioses, whereas this protein shows very low activity levels against more complex polysaccharide substrates such as β-(1,3) galactan, β-(1,3)(1,6)-galactan or arabinogalactan; no activity was found against a mix of xyloglucan oligosaccharides (Fig. 7B). The βIV-Gal presents its highest activity against β-(1,4) galactobiose but, unlike βIII-Gal, activity against β-(1,4)-galactan shows very low levels, similar to those found against lactose (Fig. 8B). Regarding the rest of linkages, the βIV-Gal showed similar activity against β-(1,3)-galactobiose and galactotriose, while lower levels of galactose are released from β-(1,−3)-galactan. Activity against β-(1,6) linkages is considerably lower and undetectable in the case of β-(1,3)(1,6)-galactan and arabinogalactan (Fig. 8B).

4. Discussion

The present work deals with two of the β-galactosidases previously identified in *Cicer arietinum,* βIII-Gal and βIV-Gal. Despite the high sequence similarity between these two proteins (Esteban et al., 2003), previous data pointed to their involvement in cell wall changes during quite different events, such as cell wall loosening for βIII-Gal (Esteban et al., 2005; Martín et al., 2005, 2013; Hernández-Nistal et al., 2014) and cell wall thickening and the cease of elongation in the case of βIV-Gal (Esteban et al., 2005; Martín et al., 2008). To deepen in the function of these β-galactosidases, transgenic arabidopsis plants overexpressing βIII-Gal and βIV-Gal, named 35S::βIII-Gal and 35S::βIV-Gal respectively, were generated and analysed.

The production in arabidopsis of the *C. arietinum* βIII-Gal does cause visible, although no drastic alterations of the morphology of the plant (Fig. 1) with respect to WT, all related to a decrease in growth at different stages of development, such as a notable decrease in the size and weight of the seedlings grown in both light and darkness (Fig. 1A-B-C), and in the diameter of the rosette (Fig. 1E) and a delay in bolting (Fig. 1F). The absence of a more severe phenotype in the studied plants

was not surprising, since similar work in potato tubers showed that overexpression of chickpea βIII-Gal (Martín et al., 2005) or a fungal endogalactanase (Sorensen et al., 2000), which resulted in an important decrease in the galactan side chains content, did not translate into a phenotypic alteration of the tubers. Likewise, the overexpression of a fungal endo β-(1,4)-galactanase in arabidopsis, with a marked decrease in the galactan side chains, only produced a slight delay in the elongation of the floral stem (Obro et al., 2009).

In our work, the observed morphological changes indicate that the action of βIII-Gal is producing changes in the cell wall characteristics contributing to a decreased growth. The FTIR spectroscopy studies results point to a lower content of galactosyl residues in the 35S::βIII-Gal plants compared to WT plants, although the most striking results are those which point to a higher representation of pectic polysaccharides, galacturonic acid and XG in these cell walls (Figs. 2 and 3 and Supplementary Fig. S3), indicating that the increase in these sugars could counteract the possible effect of galactan reduction in the cell wall by a compensation mechanism. Despite the above mentioned minor growth variations in 35S::βIII-Gal seedlings, this increase in HG and XG observed in early stages of development (3-D-old green and etiolated seedlings (Figs. 2 and 3, Supplementary Fig. S3)), could be responsible for subsequent changes in adult plants, as the delay in bolting, since both XG and HG condition cell wall dynamics, and HG has been described to determine organ initiation in Arabidopsis (Peaucelle et al., 2011).

In the previously cited works analysing the overexpression of βIII-Gal (Martín et al., 2005) or a fungal endogalactanase (Sorensen et al., 2000), the reduction in galactan side chains in potato tubers was also accompanied by an increase in the content of homogalacturonan (HG) in the first case and in the content of galacturonic acid in the second one. This conserved compensation mechanism indicates a key role of pectins, and in particular of the galactane side chains, in the mechanical properties of the cell wall.

Several studies have related galactan with the elongation capacity of the cell wall by controlling porosity or its viscoelastic properties (McCartney et al., 2000; Ha et al., 2005). The decrease of galactose or galactan chains during growth has been observed in pea epicotyls (Labavitch and Ray, 1974), in squash and *Vigna angularis* hypocotyls (Sakurai et al., 1987; Nishitani and Masuda, 1981), in alfalfa stems (Jung and Engels, 2002), or along the growth of chickpea stems (Martín et al., 2013). Similarly, during the growth of the hypocotyls of *Vigna radiata* the substitution of highly branched galactan chains for shorter chains of this polymer has been described (Hervé du Penhoat et al., 1987). Recent models of organization of the different polysaccharides in the cell wall point to a direct interaction of pectins with XG (Marcus et al., 2008; White et al., 2014), as well as interactions of the side chains of arabinan and galactan with the cellulose microfibrils (Zykwinska et al., 2007). Therefore, the reduction of galactosyl residues and the increase in the content of HG and XG in the 35S::βIII-Gal plants (Figs. 2 and 3) could be indicating an alteration of the mechanical properties of the cell wall in these plants that would explain the reduction of the growth observed in them.

The immunolabeling with galactan (LM5) specific antibody (Fig. 5A) reaffirmed the occurrence of galactan degradation during growth and by means of LM18 antibody (Fig. 5B) we confirmed the compensation in 35S::βIII-Gal transgenic plants with partially unesterified HG, indicated in the FTIR results. In the internodes of the floral stem in WT plants, a loss of galactan occurs as the elongation capacity decreases, as indicated by the decrease of LM5 labelling intensity, with a strong and homogeneous mark in the third internode weaker in the first most basal internode (Fig. 5A). In the 35S::βIII-Gal transgenic plants an evident reduction in the labelling with LM5 was observed in floral stem internodes and especially in the leaves of the rosette (Fig. 5A), still in the expansion phase, which indicates that chickpea βIII-Gal is able to hydrolyze arabidopsis cell wall galactan, as it was confirmed by the activity against β-(1,4)-galactan found in the βIII-Gal produced in *N. bentamiana* (Fig. 7A). The distribution of the label with the LM18 antibody, specific for partially unesterified HG, showed a strong increase of this polysaccharide in the 35S::βIII-Gal transgenic plants, both in leaves and in the floral stem (Fig. 5B).

The role of HG and its degree of methyl esterification in cell wall mechanical properties and extension has been extensively documented (Derbyshire et al., 2007; Röckel et al., 2008). Peaucelle et al. (2011) established that pectins are a key control point for the correct development of the organs in the apical meristem of arabidopsis, especially conditioned by the HG. Thus, the increase in the HG with low degree of methyl esterification in the 35S::βIII-Gal plants, could cause alterations of the mechanical properties of the cell wall not enough to inhibit the emergence of the floral stem, but strong enough to cause a delay in it (Fig. 1D). Similarly, the increase in HG could be responsible, together with the possible increase in XG, for the decrease in the elongation rate in the different organs studied, since both XG and HG are involved in the increase of mechanical resistance of the cell wall (Cavalier et al., 2008; Derbyshire et al., 2007).

Taking into account our present results it is evident that βIII-Gal causes a reduction of the galactan side chains in the arabidopsis cell walls which is compensated by a marked increase in homogalacturonan and XG, which allows us to attribute to galactan side chains a key role in the control of the elasticity and the correct architecture of the cell wall, and therefore in the processes of growth throughout the life of the plant. The absence of a more severe growth phenotype in 35S::βIII-Gal plants can be explained by this compensatory phenomenon in cell walls, in which the structural role of the galactan controlling the degree of porosity and therefore the accessibility of growth-controlling enzymes (Konno et al., 1986; Dopico et al., 1990; McCartney et al., 2000) or their viscoelastic properties, would be supplemented by the increase in these other polymers.

Contrary to what happens in the 35S::βIII-Gal plants, the 35S::βIV-Gal plants do not present any phenotypic changes, neither in their morphology nor in their cell walls (Figs. 4 and 6). In spite of the high degree of sequence homology between chickpea βIII-Gal and βIV-Gal proteins (81%), there are marked differences among them, such as the isoelectric points (8.06 and 5.79, respectively) or the number of putative N-glycosylation sites, one in βIII-Gal and four in βIV-Gal (Esteban et al., 2005). These differential characteristics could be conditioning the enzymatic properties of βIV-Gal, as the specificity of its substrate. We have checked by production of the βIV-Gal in a heterologous system. βIV-Gal, unlike βIII-Gal, presents very low activity against complex substrates, such as β-(1,4)-galactan, being its activity limited to very short oligosaccharides as a β-(1,4)-galactobiose. This explain the absence of changes in the level of β-(1,4) galactan and consequently the absence of changes in HG or in other polysaccharides and in the structure of the cell wall conditioning extension.

Previous works have shown that βIV-Gal protein is related to the cease of cell elongation and in chickpea is often located in cell types with thick secondary cell walls, such as xylem elements and phloem fibres (Martín et al., 2008). It has been proposed that only low molecular weight galactan is present in mature secondary cell walls, pointing to a galactan side chain reduction during cellulose microfibrill compactation (Roach et al., 2011). The substrate specificity of βIV-Gal, along with its specific location in secondary cell walls in *C. arietinum*, suggests its role in a more specific trimming of pectic galactan chains during secondary cell wall thickening, shorting side chains during the final stages of this event.

In conclusion, the fact that we observe phenotypic alterations only in the 35S:βIII-Gal plants and no in 35S::βIV-Gal, could be conditioned by the differences in the structure of these proteins, that in turn could be determining their substrate specificity or even the access to their natural substrates in the cell wall. This reflecting the distinct function of these proteins in chickpea cell walls, and could, in part, explain the differential accumulation and location patterns even within the same organs.

Funding

This work was supported by the Spanish Ministerio de Economía y Competitividad (MINECO) [grant number BFU2013-44793-P] and by the Junta de Castilla y León [grant number SA027G18].

Author statement

I Martin, B Dopico and E Labrador conceived and designed research. L Izquierdo, J Hernández-NIstal and L Albornos conducted experiments. E Labrador wrote the manuscript. P Hueso help with the enzymatic analysis of the proteins. All authors read and approved the manuscript.

Acknowledgments

We thank Dr. Toshihisa Kotake, from the Division of Life Science of Saitama University (Japan) for kindly gift of substrates, and Dr. George Lomonossoff (John Innes Centre, Norwich, UK) for pEAQ vectors development and Plant Bioscience Ltd. (Norwich, UK) for kindly providing these vectors.

Appendix A. Supplementary data

Supplementary material related to this article can be found, in the online version, at doi: https://doi.org/10.1016/j.jplph.2018.09.008.

References

Ahn, Y.O., Zheng, M., Bevan, D.R., Esen, A., Shiu, S.H., Benson, J., Peng, H.P., Miller, J.T., Cheng, C.L., Poulton, J.E., Shih, M.C., 2007. Functional genomic analysis of *Arabidopsis thaliana* glycoside hydrolase family 35. Phytochemistry 68, 1510–1520.

Albornos, L., Martín, I., Pérez, P., Marcos, R., Dopico, B., Labrador, E., 2012. Promoter activities of genes encoding β-galactosidases from Arabidopsis a1 subfamily. Plant Physiol. Biochem. 60, 223–232.

Bosch-Reig, F., Marcote, M.J., Minana, M.D., Cabello, M.L., 1992. Separation and identification of sugars and maltodextrines by thin layer chromatography: application to biological fluids and human milk. Talanta 39, 1493–1498.

Buckeridge, M.S., Reid, J.S., 1994. Purification and properties of a novel β-galactosidase or exo-(1,4)-β-D-galactanase from the cotyledons of germinated *Lupinus angustifolius* L. seeds. Planta 192, 502–511.

Cantarel, B.L., Coutinho, P.M., Rancurel, C., Bernard, T., Lombard, V., Henrissat, B., 2009. The Carbohydrate-Active EnZymes database (CAZy): an expert resource for Glycogenomics. Nucleic Acids Res. 37 (Database Issue), D233–D238.

Cavalier, D.M., Lerouxel, O., Neumetzler, L., Yamauchi, K., Reinecke, A., Freshour, G., 2008. Disrupting two *Arabidopsis thaliana* xylosyltransferase genes results in plants deficient in xyloglucan, a major primary cell wall component. Plant Cell 20, 1519–1537.

Černá, M., Barros, A.S., Nunes, A., Rocha, S.M., Delgadillo, I., Copiková, J., Coimbra, M.A., 2003. Use of FT-IR spectroscopy as a tool for the analysis of polysaccharide food additives. Carbohydr. Polym. 51, 383–389.

Clough, S.J., Bent, A.F., 1998. Floral dip: a simplified method for *Agrobacterium*-mediated transformation of *Arabidopsis thaliana*. Plant J. 16, 735–743.

Derbyshire, P., McCann, M.C., Roberts, K., 2007. Restricted cell elongation in arabidopsis hypocotyls is associated with a reduced average pectin esterification level. BMC Plant Biol. 7, 31.

Dopico, B., Nicolás, G., Labrador, E., 1989. Partial purification of cell wall β-galactosidases from *Cicer arietinum* epicotyls. Relationship with cell wall autolytic processes. Physiol. Plant. 75, 458–464.

Dopico, B., Nicolás, G., Labrador, E., 1990. Changes during epicotyl growth of an autolysis-related β-galactosidase from the cell wall of *Cicer arietinum*. Plant Sci. 72, 45–51.

Edwards, M., Bowman, J.L., Dea, I.C.M., Reid, J.S.G., 1988. A β-D-galactosidase from nasturtium (*Tropaeolum majus* L.) cotyledons. J. Biol. Chem. 263, 4333–4337.

Esteban, R., Dopico, B., Muñoz, F.J., Romo, S., Martín, I., Labrador, E., 2003. Cloning of a *Cicer arietinum* β-galactosidase with pectin–degrading function. Plant Cell Physiol. 44, 718–725.

Esteban, R., Labrador, E., Dopico, B., 2005. A family of β-galactosidase cDNAs related to development of vegetative tissue in Cicer arietinum. Plant Sci. 168, 457–466.

Ha, M.A., Viëtor, R.J., Jardine, G.D., Apperley, D.C., Jarvis, M.C., 2005. Conformation and mobility of the arabinan and galactan side-chains of pectin. Phytochemisrty 66, 1817–1824.

Hernández-Nistal, J., Martín, I., Dopico, B., Labrador, E., 2014. Coordinated action of β-galactosidases in the cell wall of embryonic axes during chickpea germination and seedling growth. Plant Biol. 16, 404–410.

Hervé du Penhoat, C., Michon, V., Goldberg, R., 1987. Development of arabinans and galactans during the maturation of hypocotyls cells of mung bean (*Vigna radiata* Wilzech). Carbohydr. Res. 166, 31–42.

Hobson, N., Deyholos, M.K., 2013. Genomic and expresion analysis of the flax (*Linum usitatissimum*) family of glycosyl hidrolase 35 genes. BMC Genomics 14, 344.

Jones, L., Seymour, G.B., Knox, J.P., 1997. Localization of pectic galactan in tomato cell walls using a monoclonal antibody specific to (1–4)-β-D-galactan. Plant Physiol. 113 1505-1412.

Jung, H.G., Engels, F.M., 2002. Alfalfa stem tissues. Crop Sci. 42, 524–534.

Kacuráková, M., Capek, P., Sasinková, V., Wellner, N., Ebringerová, A., 2000. FTIR study of plant cell wall model compounds: pectic polysaccharides and hemicelluloses. Carbohydr. Polym. 43, 195–203.

Konno, H., Yamasaki, Y., Katoh, K., 1986. Characteristics of β-galactosidase purified from suspension cultures of carrot. Physiol. Plant. 68, 46–52.

Kooiman, P., 1960. A method for the determination of amyloid in plant seeds. Recl. Trav. Chim. Pays Bas 79, 675–678.

Kotake, T., Dina, S., Konishi, T., Kaneko, S., Igarashi, K., Samejima, M., Watanabe, Y., Kimura, K., Tsumuraya, Y., 2005. Molecular cloning of a β-galactosidase from radish that specifically hydrolyzes β-(1-3)- and β-(1-6)-galactosyl residues of arabinogalactan protein. Plant Physiol. 138, 1563–1576.

Labavitch, J.M., Ray, P.M., 1974. Turnover of cell wall polysaccharides in elongating pea stem segments. Plant Physiol. 53, 669–673.

Liu, J., Gao, M., Lv, M., Cao, J., 2013. Structure, evolution, and expression of the β-galactosidase gene family in *Brassica campestris* ssp. *chinensis*. Plant Mol. Biol. Rep. 31, 1249–1260.

Marcus, S.E., Verhertbruggen, Y., Hervé, C., Ordaz-Ortiz, J.J., Farkas, V., Pedersen, H.L., Willats, W.G.T., Knox, J.P., 2008. Pectic homogalacturonan mask abundant set of xyloglucan epitopes in plant cell walls. BMC Plant Biol. 8, 60.

Martín, I., Dopico, B., Muñoz, F.J., Esteban, R., Oomen, R.J.F.J., Driouich, A., Vincken, J.P., Visser, R., Labrador, E., 2005. *In vivo* expression of a *Cicer arietinum* β-galactosidase in potato tubers leads to a reduction of the galactan side-chains in cell wall pectin. Plant Cell Physiol. 46, 1613–1622.

Martín, I., Jiménez, T., Esteban, R., Dopico, B., Labrador, E., 2008. Immunolocalization of a cell wall β-galactosidase reveals its developmentally regulated expression in *Cicer arietinum* and its relationship to vascular tissue. J. Plant Growth Regul. 27, 181–191.

Martín, I., Jiménez, T., Hernández-Nistal, J., Labrador, E., Dopico, B., 2009. The location of the chickpea cell wall βV-galactosidase suggests involvement in the transition between cell proliferation and cell elongation. J. Plant Growth Regul. 28, 1–11.

Martín, I., Jiménez, T., Hernández-Nistal, J., Dopico, B., Labrador, E., 2011. The βI-galactosidase of *Cicer arietinum* is located in thickened cell walls such as those of collenchyma, sclerenchyma and vascular tissue. Plant Biol. 13, 777–783.

Martín, I., Hernández-Nistal, J., Albornos, L., Labrador, E., Dopico, B., 2013. βIII-Gal is involved in galactan reduction during phloem element differentiation in chickpea stems. Plant Cell Physiol. 54, 960–970.

McCann, M.C., Chen, L., Roberts, K., Kemsley, E.K., Sene, C., Carpita, N.C., Stacey, N.J., Wilson, R.H., 1997. Infrared microspectroscopy: sampling heterogeneity in plant cell wall composition and architecture. Physiol. Plant. 100, 729–738.

McCartney, L., Ormerod, A.P., Gidley, M.J., Knox, J.P., 2000. Temporal and spatial regulation of pectic (1-4)-β-D-galactan in cell walls of developing pea cotyledons: implications for mechanical properties. Plant J. 22, 105–113.

McCartney, L., Steele-King, C.G., Jordan, E., Knox, J.P., 2003. Cell wall pectic (1-4)-β-D-galactan marks the acceleration of cell elongation in the Arabidopsis seedling root meristem. Plant J. 33, 447–454.

Moneo-Sánchez, M., Izquierdo, L., Martín, I., Hernández-Nistal, J., Albornos, L., Dopico, B., Labrador, E., 2018. Knockout mutants of *Arabidopsis thaliana* β-galactosidase. Modifications in the cell wall saccharides and enzymatic activities. Biol. Plant. 62, 80–88.

Morris, V.J., Ring, S.G., MacDougall, A.J., Wilson, R.H., 2003. Biophysical characterisation of plant cell walls. In: Rose, J. (Ed.), The Plant Cell Wall. Annual Plant Reviews. Blackwell Publishing, Oxford, pp. 55–91.

Murashige, T., Skoog, F., 1962. A revised medium for rapid growth and bioassays with tobacco tissue cultures. Physiol. Plant. 15, 473–497.

Nishitani, K., Masuda, Y., 1981. Auxin-induced changes in the cell wall structure: changes in the sugar compositions, intrinsic viscosity and molecular weight distributions of matrix polysaccharides of the epicotyl cell wall of *Vigna angularis*. Physiol. Plant. 52, 482–494.

Obro, J., Borkhardt, B., Harholt, J., Skjøt, M., Willats, W.G., Ulvskov, P., 2009. Simultaneous in vivo truncation of pectic side chains. Transgenic Res. 18, 961–969.

Peaucelle, A., Braybrook, S.A., Le Guillou, L., Bron, E., Kuhlemeier, C., Höfte, H., 2011. Pectin-induced changes in cell wall mechanics underlie organ initiation in Arabidopsis. Curr. Biol. 21, 1720–1726.

Roach, M.J., Mokshina, N.Y., Badhan, A., Snegireva, A.V., Hobson, N., Deyholos, M.K., Gorshkova, T.A., 2011. Development of cellulosic secondary walls in flax fibers requires beta-galactosidase. Plant Physiol. 156, 1351–1363.

Röckel, N., Wolf, S., Kost, B., Rausch, T., Greiner, S., 2008. Elaborate spatial patterning of cell-wall PME and PMEI at the pollen tube tip involves PMEI endocytosis, and reflects the distribution of esterified and de-esterified pectins. Plant J. 53, 133–143.

Ross, G.S., Wegrzyn, T., MacRae, E.A., Redgwell, R.J., 1994. Apple β-galactosidase. Activity against cell wall polysaccharides and characterization of a related cDNA clone. Plant Physiol. 106, 521–528.

Sainsbury, F., Thuenemann, E.C., Lomonossoff, G.P., 2009. PEAQ: versatile expression vectors for easy and quick transient expression of heterologous proteins in plants. Plant Biotechnol. J. 7, 682–693.

Sakurai, N., Tanaka, S., Kuraishi, S., 1987. Changes in wall polysaccharides of squash (*Cucurbita maxima* Duch.) hypocotyls under water stress condition. II. Composition of pectic and hemicellulosic polysaccharides. Plant Cell Physiol. 28, 1059–1070.

Sampedro, J., Gianzo, C., Iglesias, N., Guitián, E., Revilla, G., Zarra, I., 2012. AtBGAL10 is the main xyloglucan β-galactosidase in arabidopsis, and its absence resuls in unusual xyloglucan subunits and growth defects. Plant Physiol. 158, 1146–1157.

Smith, L.D., Gross, K.C., 2000. A family of at least seven β-galactosidase genes is

expressed during tomato fruit development. Plant Physiol. 123, 1173–1183.
Sorensen, S.O., Pauly, M., Bush, M., Skjot, M., McCann, M.C., Borkhardt, B., Ulvskov, P., 2000. Pectin engineering: modification of potato pectin by in vivo expression of an endo-1, 4-β-D-galactanase. Proc. Natl. Acad. Sci. U. S. A. 97, 7639–7644.
White, P.B., Wang, T., Park, Y.B., Cosgrove, D.J., Hong, M., 2014. Water-polysaccharide interactions in the primary cell wall of *Arabidopsis thaliana* from Polarization Transfer Solid-State NMR. J. Am. Chem. Soc. 136, 10399–10409.
Wu, Z., Burns, J.K., 2004. A β-galactosidase gene is expressed during mature fruit abscission in' Valencia' orange (*Citrus sinensis*). J. Exp. Bot. 55, 1483–1490.
Zykwinska, A., Thibault, J.F., Ralet, M.C., 2007. Organization of pectic arabinan and galactan side chains in association with cellulose microfibrils in primary cell walls and related models envisaged. J. Exp. Bot. 58, 1795–1802.